

AN EXPLANATION FOR THE OBSERVED WEAK SIZE EVOLUTION OF DISK GALAXIES

RACHEL S. SOMERVILLE¹, MARCO BARDEN¹, HANS-WALTER RIX¹, ERIC F. BELL¹, ANDREA BORCH^{1,2}, STEVEN V. W. BECKWITH^{3,4}, JOHN A. R. CALDWELL⁵, BORIS HÄUSSLER¹, CATHERINE HEYMANS⁶, KNUD JAHNKE¹, SHARDHA JOGEE⁷, DANIEL H. MCINTOSH⁸, KLAUS MEISENHEIMER¹, CHIEN Y. PENG³, SEBASTIAN F. SÁNCHEZ⁹, LUTZ WISOTZKI¹⁰, CHRISTIAN WOLF¹¹

Draft version December 2, 2024

ABSTRACT

Surveys of distant galaxies with the Hubble Space Telescope and from the ground have shown that there is only mild evolution in the relationship between radial size and stellar mass for galactic disks from $z \sim 1$ to the present day. Using a sample of nearby disk-dominated galaxies from the Sloan Digital Sky Survey (SDSS), and high redshift data from the GEMS (Galaxy Evolution from Morphology and SEDs) survey, we investigate whether this result is consistent with theoretical expectations within the hierarchical paradigm of structure formation. The radius-mass relation for virialized dark matter halos in the Λ CDM model evolves by about a factor of two over this interval. However, high resolution N-body simulations have shown that dark matter halos in hierarchical models build up from the inside out, so that the inner part of the halo, where the baryons are concentrated, changes very little over this interval. We compute the expected disk size-stellar mass distribution, accounting for this evolution in the internal structure of dark matter halos and the adiabatic contraction of the dark matter by the self-gravity of the collapsing baryons. We find that the predicted evolution in the mean size at fixed stellar mass since $z \sim 1$ is about 15–20 percent, in good agreement with the observational constraints from GEMS. At redshift $z \sim 2$, the model predicts that disks at fixed stellar mass were on average only 60% as large as they are today. This is somewhat stronger evolution than the available observations indicate, but is consistent with the data within the uncertainties.

Subject headings: galaxies: spiral – galaxies: evolution – galaxies: high redshift – surveys – cosmology: observations

1. INTRODUCTION

The relationship between the radial size and the luminosity or stellar mass of galactic disks is a fundamental scaling relation that reveals important aspects of the formation history of these objects. The size, luminosity/mass, and rotation velocity form a ‘fundamental plane’ for disks at the present epoch (Pizagno et al. 2006) that is analogous to the more familiar fundamental plane for early-type galaxies (Burstein et al. 1997). The zero-point, slope, and scatter of the fundamental plane for both disks and spheroids, and the evolution of these quantities over cosmic time, pose strong constraints on

Electronic address: somerville@mpia.de

¹ Max-Planck-Institut für Astronomie, Königstuhl 17, Heidelberg, 69117, Germany

² Astronomisches Rechen-Institut, Mönchhofstr. 12-14, D-69120, Heidelberg, Germany

³ Space Telescope Science Institute, 3700 San Martin Dr., Baltimore, MD 21218, USA

⁴ Johns Hopkins University, 3400 North Charles Street, Baltimore, MD 21218, USA

⁵ University of Texas, McDonald Observatory, Fort Davis, TX 79734

⁶ Department of Physics and Astronomy, University of British Columbia, 6224 Agricultural Road, Vancouver, V6T 1Z1, Canada

⁷ Department of Astronomy, University of Texas at Austin, 1 University Station, C1400 Austin, TX 78712-0259, USA

⁸ Department of Astronomy, University of Massachusetts, 710 North Pleasant Street, Amherst, MA 01003, USA

⁹ Centro Hispano Alemán de Calar Alto, C/Jesus Durban Remón 2-2, Almería, E-04004, Spain

¹⁰ Astrophysikalisches Institut Potsdam, An der Sternwarte 16, Potsdam, 14482, Germany

¹¹ Department of Physics, Denys Wilkinson Bldg., University of Oxford, Keble Road, Oxford, OX1 3RH, UK

models of galaxy formation.

In the Cold Dark Matter (CDM) paradigm, dark matter (DM) and gas acquire angular momentum via tidal torques in the early universe (Peebles 1969). When the gas cools and condenses, this angular momentum may eventually halt the collapse and lead to the formation of a rotationally supported disk (Fall & Efstathiou 1980). Under the assumption that the specific angular momentum of the pre-collapse gas is similar to that of the DM and is mostly conserved during collapse, this picture leads to predictions of present-day disk sizes that are in reasonably good agreement with observations (Kauffmann 1996; Dalcanton et al. 1997; Mo et al. 1998; Avila-Reese et al. 1998; Somerville & Primack 1999; van den Bosch 2000).

However, in detailed numerical hydrodynamic simulations of disk formation in a CDM universe, the proto-disk gas tends to lose a large fraction of its angular momentum via mergers, leading to disks that are too small and compact (Navarro & White 1994; Sommer-Larsen et al. 1999; Navarro & Steinmetz 2000). It is still not clear whether this problem reflects a fundamental problem with CDM (i.e., excess small scale power), or is due to inadequate numerical resolution or treatment of “gastrophysical” processes like star formation and feedback (Governato et al. 2004; Robertson et al. 2004). However, it has been suggested that delayed cooling and star formation, perhaps due to strong feedback in low-mass progenitors, could help to alleviate this problem (Weil et al. 1998; Maller & Dekel 2002). The observed evolution of disk scaling relations at high redshift can provide important constraints on such scenarios.

The observational relationship between radial size (effective radius or disk scale length) and luminosity or stellar mass for disks at low redshift has now been well-characterized by studies based on the Sloan Digital Sky Survey (SDSS; e.g. Shen et al. 2003, hereafter S03). Several pioneering studies in the past decade have studied the size-luminosity relation for disks out to redshift $z \sim 1$ (e.g. Lilly et al. 1998; Simard et al. 1999). Lilly et al. (1998) concluded that the surface brightness of disk galaxies at $z \sim 1$ were about 1 magnitude brighter than present-day disks. Simard et al. (1999) concluded that, when the impact of surface brightness selection effects was taken into account, there was less than 0.4 mag arcsec $^{-1}$ of evolution over the same redshift range. Sizes were also measured for Lyman Break Galaxies (LBGs) at redshifts $z \sim 3$ (Giavalisco et al. 1996; Lowenthal et al. 1997), but these results were difficult to compare with low redshift galaxies because both the luminosities and sizes were measured in the rest-UV rather than the optical.

Recently, new studies with the Advanced Camera for Surveys (ACS) on the Hubble Space Telescope (HST) have provided greatly improved constraints on the disk size-luminosity relation at high redshift. Ravindranath et al. (2004) and Ferguson et al. (2004) presented size distributions for $z \lesssim 1$ disk-type galaxies and for rest-UV selected galaxies from $1.4 \lesssim z \lesssim 6$, respectively, based on samples selected from the Great Observatories Origins Deep Survey (GOODS). Barden et al. (2005, hereafter B05) presented the luminosity-size and stellar mass-size relation out to $z \sim 1$ based on the GEMS (Galaxy Evolution from Morphology and SEDs) survey (Rix et al. 2004). They concluded that disk galaxies of a given size at $z \sim 1$ are ~ 1 magnitude brighter in the V -band, but that there is less than about a ten percent change in the *stellar mass* at a given size between $z \sim 1$ and the present. This is consistent with a mean stellar mass-to-light ratio that increases with time, as expected based on the simple aging of stellar populations. Trujillo et al. (2004) measured luminosity-size and stellar mass-size relations in the rest-frame optical (based on the ground-based Near Infrared selected FIRE sample) out to $z \sim 2.5$, and found that the average surface brightness at $z \sim 2.5$ is about 2–3 mag arcsec $^{-1}$ brighter than in the local universe, but the average size at a fixed stellar mass has evolved by less than a factor of two. Trujillo et al. (2006, hereafter T06) presented the results of a similar analysis of a larger sample from FIRE, and combined those results with the lower redshift studies of S03 and B05.

In the very simplest version of the Fall-Efstathiou picture, we expect the size of a galactic disk that forms within a dark matter halo to scale as $r_{\text{disk}} \propto \lambda r_{\text{vir}}$, where λ is the dimensionless spin parameter and r_{vir} is the virial radius of the dark matter halo. N-body simulations have demonstrated that the spins of dark matter halos are not correlated with halo mass or most other properties, and the distribution does not evolve with time (e.g. Bullock et al. 2001a). If the stellar mass of the disk is a constant fraction of the halo virial mass, then, the most naïve expectation is that the average size of galactic disks of a given stellar mass will evolve as r_{vir} evolves for halos of a given virial mass. In the currently favored Λ CDM

cosmology, this implies an evolution of a factor of ~ 1.7 out to $z = 1$ and a factor of ~ 3.2 out to $z \sim 3$. This simple $r_{\text{disk}} \propto \lambda r_{\text{vir}}$ scaling has frequently been used in the literature as a theoretical baseline (e.g. Mao et al. 1998; Ferguson et al. 2004, B05, T06). Mao et al. (1998) found that this naïve scaling was consistent with the size evolution of disks out to $z \sim 1$ compared with the data available at the time, but the samples were tiny, and the observational selection effects were not well characterized or accounted for. Ferguson et al. (2004) found that the average rest-UV sizes of rest-UV selected galaxies at $1.4 \lesssim z \lesssim 5$ were consistent with this scaling. Most recently, B05 and T06 concluded that the predicted evolution in this scenario is considerably stronger than the observed evolution of the rest-optical sizes in their stellar-mass selected disk samples.

However, this simple scaling neglects several important factors that are believed to play a role in determining the size of galactic disks forming in CDM halos. 1) The mass density profiles of CDM halos have a universal form (known as the Navarro-Frenk-White (NFW) profile; Navarro et al. 1997), characterized by the concentration parameter c_{NFW} . The concentration parameter quantifies the density of the halo on small (\sim kpc) scales relative to the virial radius, and has an important impact on the structural parameters of the resulting disk. There is a correlation between halo virial mass M_{vir} and concentration (Navarro et al. 1997), though with a significant scatter (Bullock et al. 2001b), and this mean halo concentration-mass relation evolves with time, in the sense that halos of a given mass were less concentrated in the past (Bullock et al. 2001b). 2) The self-gravity of the baryonic material may modify the distribution of the dark matter as it becomes condensed in the central part of the halo (“adiabatic contraction”) 3) Disks with low values of λ and/or large baryonic-to-dark mass ratios may not have sufficient angular momentum to support a stable disk. These unstable disks may form a bar or a bulge, and might no longer be included in a sample of ‘disk dominated’ galaxies.

There are of course numerous other potential complications in the process of the formation and evolution of galactic disks, which we do not consider here (though we discuss some of them in §5). We present the predictions of a simple ‘first order’ model for disk formation, which is set within the CDM framework, and which incorporates cosmological NFW halo profiles, adiabatic contraction, and disk instability. This model is based on the formalism and basic ingredients presented in Blumenthal et al. (1986), Flores et al. (1993), and Mo et al. (1998, MMW98). Our primary goal is to determine whether these predictions are compatible with the rather weak observed evolution of the disk stellar mass-size relation out to $z \sim 1$ reported by B05. We also extend these predictions out to higher redshift $z \sim 3$, and compare with the results reported by T06.

We discuss the ingredients of our model in §2, give a brief summary of the observational data in §3, present our results in §4, and discuss our results and conclude in §5. We assume the following values for the cosmological parameters: matter density $\Omega_m = 0.3$, baryon density $\Omega_b = 0.044$, cosmological constant $\Omega_\Lambda = 0.70$, Hubble parameter $H_0 = 70 \text{ km s}^{-1} \text{ Mpc}^{-1}$, fluctuation amplitude $\sigma_8 = 0.9$, and a scale-free primordial power spectrum

$$n_s = 1.$$

2. MODEL

Over a given redshift interval, we select halo masses from the mass function of Sheth & Tormen (1999) using a Monte Carlo procedure. We assume that each halo with a circular velocity below 350 km/s hosts one disk galaxy at its center. Each halo is assigned a spin λ selected from a log-normal distribution with mean $\bar{\lambda} = 0.05$ and width $\sigma_\lambda = 0.5$ (Bullock et al. 2001a). Note that as in Somerville & Primack (1999) and Bullock et al. (2001b) we define virial masses, velocities, and radii within the virial overdensity Δ_{vir} with respect to the *mean* matter density of the universe, rather than within an overdensity of 200 with respect to the *critical* density as in MMW98 and NFW (in our adopted cosmology, $\Delta_{\text{vir}}(z=0) \simeq 337$). It is important to note that the numerical values of circular velocity, radius, and concentration for a halo of a given mass, as well as the implied redshift evolution of these quantities, depend non-trivially on this choice of definition, although it is somewhat arbitrary and several conventions are practiced in the literature. We assume that initially the halo mass density profiles obey the Navarro-Frenk-White form (Navarro et al. 1997), and compute the halo concentration as a function of mass and redshift using the analytic fitting functions provided by Bullock et al. (2001b). We assume that a fraction $f_d \equiv m_d/M_h$ of the halo mass is in the form of baryons that are able to cool and collapse, forming a disk with mass m_d . Following S03, we assume that f_d is a function of halo mass, described by the simple functional form: $f_d = f_0/[1.0 + (M_h/M_c)^\alpha]$, with $f_0 = 0.13$, $M_c = 1.0 \times 10^{12} M_\odot$, and $\alpha = -0.67$. This scaling of f_d with halo mass is chosen in order to reproduce the observed relationship between stellar mass and disk scale radius at $z \sim 0$ (in particular, earlier models that assumed a constant value of f_d for all halos are not able to reproduce the slope of the r_s - m_* relation; S03). We do not discriminate between stellar mass and the mass in cold gas. For the relatively massive disks that we will focus on, the cold gas fraction should be fairly low.

The specific angular momentum of the disk material is related to that of the halo via the parameter $f_j \equiv J_d/J_h$, where J_d is the angular momentum of the disk and J_h is the angular momentum of the halo. We assume $f_j = 1$, i.e., that the specific angular momentum of the disk is the same as that of the dark matter halo. We compute the size and maximum circular velocity of the resulting disk, including the adiabatic contraction of the halo, using a method similar to that outlined in MMW98. As in MMW98, we consider the possibility that disks with $\epsilon_m \equiv V_{\text{max}}/(Gm_d/r_d)^{1/2}$ less than a critical value $\epsilon_{m,\text{crit}}$ may be unstable to the formation of a bar and/or bulge. We repeat our analysis with these objects excluded.

3. SUMMARY OF OBSERVATIONAL DATA

For the main part of our analysis, we use the same sample of disk-dominated galaxies that was used for the analysis of B05. We give a brief summary of that sample here, and refer to B05 for details. For our local $z \sim 0$ sample, we use the NYU Value-added Galaxy Catalog (VAGC; Blanton et al. 2005), based on the second data release of the SDSS (DR2). The VAGC catalog was used to obtain Sérsic parameters, r -band half-light

radii, and magnitudes. We then construct a sample of disk-dominated galaxies by requiring Sérsic parameter $n < 2.5$. We convert the r -band half-light radii to rest-frame V -band radii using the conversion derived in B05, $R_e(V) = 1.011R_e(r)$. We compute stellar masses from the (k-corrected) g and r -band photometry, using the prescription of Bell et al. (2003), which relies on a conversion between $g - r$ color and average stellar mass-to-light ratio. We assume a normalization for this relation consistent with a Kroupa (2001) IMF.

Our high redshift disk sample comes from the GEMS survey (Rix et al. 2004), which consists of V_{606} and z_{850} imaging over an area of ~ 900 arcmin 2 with the ACS on HST. The 5σ point source detection limit is 28.3 magnitude in the V_{606} band and 27.1 magnitude in z_{850} . The GEMS object catalog is based on the z_{850} image; for details see Caldwell et al. (2006). High-accuracy photometric redshift estimates ($\sigma_z/(z+1) \sim 0.02$) are obtained from the ground-based COMBO-17 survey (Wolf et al. 2004). The R -band selection limit of COMBO-17 ($m_R \sim 24$) limits the range of the sample to redshifts $z \lesssim 1$. The 17-band photometry of COMBO has also been used to obtain stellar mass estimates (Borch et al. 2006), assuming a Kroupa IMF. The GEMS main sample consists of almost 8000 galaxies with COMBO counterparts and redshifts. We fit each galaxy with a Sérsic profile and select a disk-dominated sample with good quality fits, Sérsic $n < 2.5$, and extended light profiles. This sample contains 5664 objects. Typical uncertainties are $\sim 35\%$ in r_e and ~ 0.2 magnitudes in m_z . The apparent half-light sizes measured in the observed z_{850} band are converted to rest-frame V -band using an average color gradient correction based on a local sample of disk galaxies (see B05). These corrections are small ($\pm 3\%$) over the entire redshift range of our sample (the observed z_{850} band samples the rest-frame V -band at $z \sim 0.5$). Where disk scale radii are quoted in this work, we have obtained them by simply assuming that the measured half-light radius and the disk scale radius are related by the standard expression for a pure exponential disk, $r_d = r_e/1.68$.

In order to estimate the completeness of the combined GEMS+COMBO disk sample, we have performed extensive simulations (Häussler et al. 2006; Rix et al. 2004). Artificial disks were inserted into blank sky, and the source detection and fitting software was run on this image. Poor fits are excluded in the same manner as for the real galaxy images. We can then calculate the success rate for detecting and obtaining a good fit for the artificial galaxies, as a function of apparent effective radius and apparent magnitude. We multiply this GEMS completeness factor by the (redshift, magnitude, and color-dependent) probability that the galaxy would be detected and successfully assigned a redshift in the COMBO survey. Based on these estimates, B05 argue that GEMS is not surface brightness limited even in the highest redshift bin, and that the combined GEMS+COMBO sample is complete down to stellar masses of $10^{10} M_\odot$. As in B05, we limit our analysis to galaxies with stellar mass greater than this value, and we weigh galaxies by the inverse completeness factor in computing distributions and means. To avoid using galaxies with very large weights, we exclude objects with a completeness factor smaller than 0.5. B05 have shown

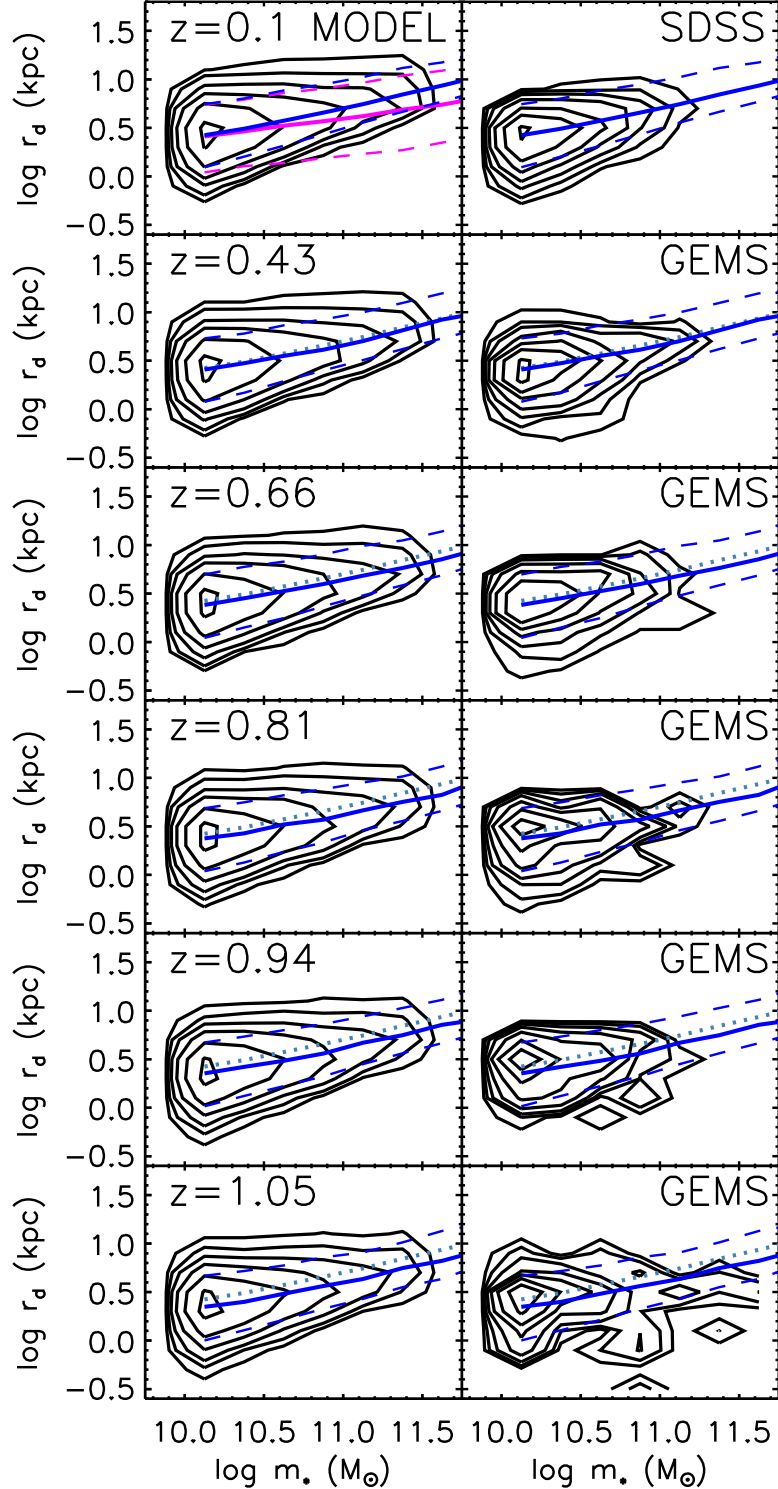


FIG. 1.— The relationship between stellar mass and disk scale length for a “local” sample ($0.001 < z < 0.2$) and in five redshift bins of approximately equal comoving volume from $z = 0.1$ to $z = 1.1$. In the left panels, contours show the model predictions for *stable* disks. In the right panels, contours show the completeness-corrected distributions for the SDSS and GEMS samples for the same redshift bins. The left and right panels are normalized to the same total number density in each redshift bin. The dark blue solid and dashed lines show the median and 10 and 90th percentiles, respectively, for the stable *model* disks *in both columns of panels* (models and data). The magenta solid and dashed lines in the left $z = 0.1$ panel show the median and 10 and 90th percentiles for all disks, without any stability criterion applied. The gray-blue dotted lines, repeated in each panel, show the $z = 0.1$ medians and 10 and 90 percentile lines for the stable model disks.

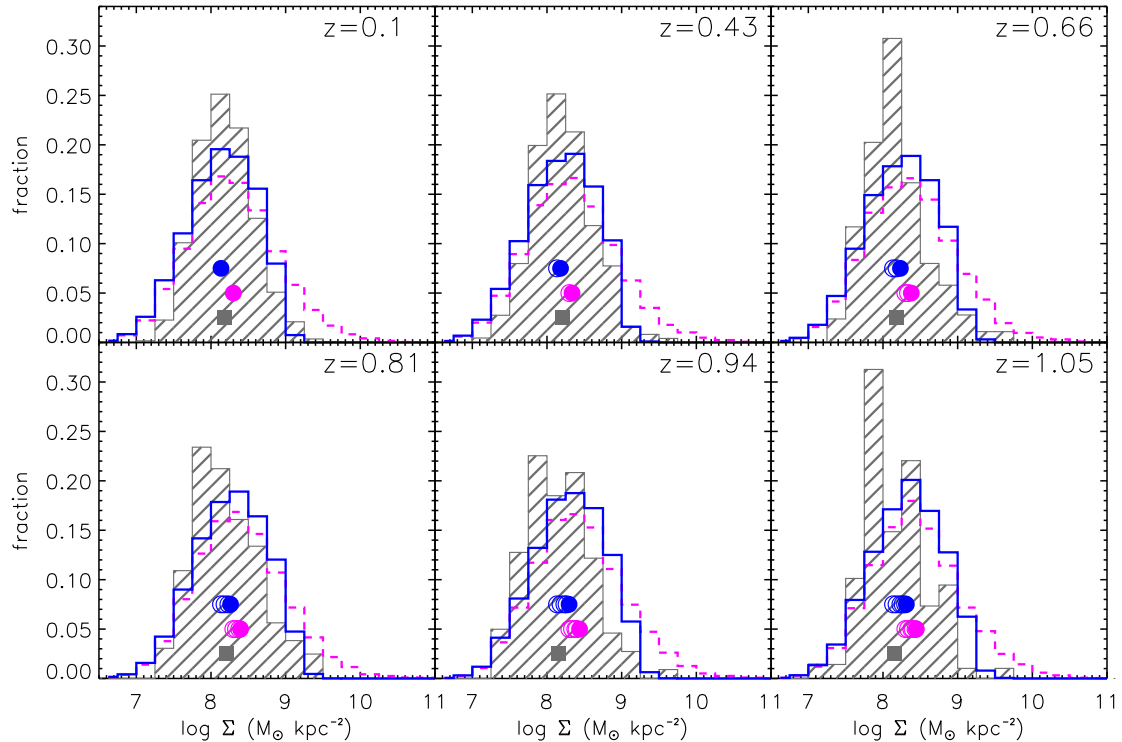


FIG. 2.— The distribution of stellar surface densities for disks with stellar mass $10^{10} M_{\odot} < m_* < 10^{11} M_{\odot}$, for a “local” sample ($0.001 < z < 0.2$), and in five redshift bins of approximately equal comoving volume from $z = 0.1$ to $z = 1.1$. Shaded histograms show the completeness-corrected distributions of SDSS and GEMS disks, selected via Sérsic fits to their radial light profiles ($n < 2.5$). Solid squares show the mean value of $\log \Sigma_*$ derived from these observations. Magenta dashed lines show the distributions for all model disks, and dark blue solid lines show the results for “stable” model disks only (see text). The solid dots indicate the mean of the model distribution for the current redshift bin, and the open dots show the means from all lower redshift bins. The upper set of dark blue dots are for stable disks, and the lower set of magenta dots are for all disks.

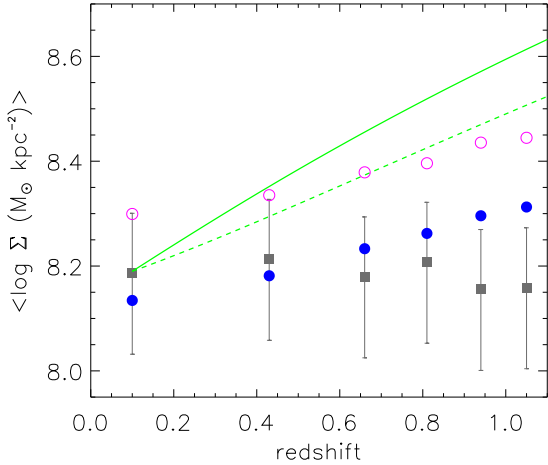


FIG. 3.— The redshift evolution of the mean stellar surface density. Solid squares show the mean of $\log \Sigma_*$ for SDSS and GEMS disks with $10^{10} M_\odot < m_* < 10^{11} M_\odot$. Open magenta dots show the results for all model disks in this mass range, and solid blue dots show the results for stable model disks only. The dashed curve shows the evolution in Σ_* that we would expect if disk size scaled like r_{200} , and the solid curve shows the evolution for disk sizes that scale like r_{vir} (see text).

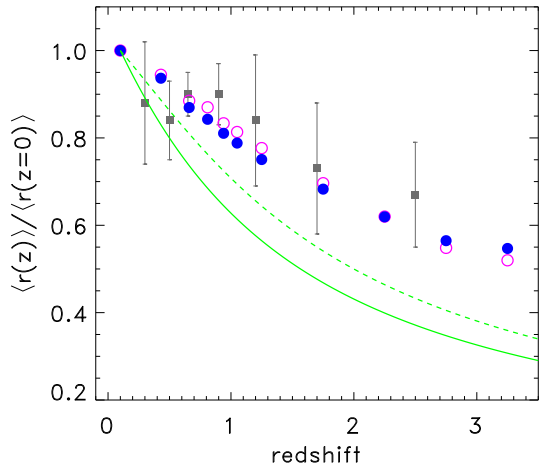


FIG. 4.— The redshift evolution of the average size of disks with stellar masses greater than $3 \times 10^{10} M_\odot$, relative to the average size of disks at $z = 0.1$. Square symbols with error bars show the observational estimates from T06, obtained by combining the SDSS, GEMS, and FIRES datasets. Open (magenta) dots show the model predictions for all disks. Solid (dark blue) dots show the model predictions for stable disks only. The green dashed and solid curves show the scaling of r_{200} and r_{vir} (respectively) for dark matter halos of fixed mass.

that the average sizes and surface densities are insensitive to the choice of this limiting completeness factor at our adopted stellar mass limit.

4. RESULTS

Using the models outlined above, we construct a mock catalog for a low redshift slice ($0.001 < z < 0.2$) repre-

sentative of the SDSS sample, as well as a lightcone from $0.1 < z < 1.1$ with approximately ten times the area of GEMS ($10 \times 900 \text{ arcmin}^2$), which we divide into five bins with roughly equal comoving volume ($0.1 < z < 0.56$, $0.56 < z < 0.74$, $0.74 < z < 0.87$, $0.87 < z < 1.0$, $1.0 < z < 1.1$). Following MMW98, we define “stable disks” as those with stability parameter ϵ_m above a critical value, and adopt $\epsilon_{m,\text{crit}} = 0.75$ (Syer et al. 1999). The stellar mass vs. disk scale length relations for the six redshift bins from $z \sim 0$ –1 are shown in Figure 1, for the mock catalogs on the left and the observed SDSS and GEMS disk samples on the right¹². The observational samples are corrected for completeness as described above. In the left panels of Fig. 1, the contours show the results for *stable disks* only. To illustrate the impact of excluding the unstable disks, the median and 10 and 90th percentiles in size as a function of stellar mass for all disks, without any stability criterion applied, are shown in the $z = 0.1$ panel. The relative impact of applying the stability criterion on the size-mass relation and its scatter is similar in all the redshift bins considered here, so for clarity we show only the median relation for stable disks in the other panels. It is clear from the definition of the stability parameter ϵ_m that at a given halo mass, disks with larger values of f_d are more likely to be unstable, and also at a given stellar mass, more compact disks (low r_d) are more likely to be unstable. Therefore, more massive galaxies are more likely to be unstable (recall that we assumed that f_d increases with increasing halo mass), and so excluding the unstable (compact) disks results in a steepening of the slope in the $m_* - r_d$ relation at $m_* \simeq 2 - 3 \times 10^{10} M_\odot$. Excluding the unstable disks also significantly reduces the scatter in disk size at fixed stellar mass for the massive disks. The fraction of disks deemed stable by our criterion is nearly constant over the redshift range considered here, and ranges from 95% at $z \sim 0.1$ to 97% at $z \sim 1$.

From Figure 1 we see that, in agreement with S03 and other investigations, this rather simple model can reproduce the observed slope of the size-mass relation and the observed scatter in size at a given stellar mass fairly well at $z \sim 0$. The median and 10 and 90th percentiles in disk scale length as a function of stellar mass for the stable model disks from the low redshift bin are repeated in every panel, and from this we can immediately see that the model predicts that the average size of disks at fixed stellar mass has increased by about 15–20% since $z \sim 1$. The GEMS sample appears consistent with no evolution in size at fixed stellar mass. Note that we have normalized the model and data histograms to the same total number density in each redshift bin.

Figure 2 shows the distribution of stellar surface densities Σ_* for the same six redshift bins from $z \sim 0.1$ to $z \sim 1$. An important side issue is that we could see in Figure 1 that the model produces too many massive disks ($m_* > 10^{11} M_\odot$), especially at high redshift, compared with the observational samples. This is hardly surpris-

¹² Note that, strictly speaking, the models predict the scale length of the *baryonic mass* in the disk, while the observed scale lengths are for the rest-frame *V*-band light. We do not attempt to correct for the known $\sim 20\%$ difference between these two quantities, since we are mainly interested in the redshift evolution. We do note here, however, that time-evolving color gradients could therefore change our results.

ing, since we have assumed that *every* dark matter halo contains a single disk galaxy, which is clearly not realistic, and we know that more massive halos (which produce the massive disks) are more likely to instead host an early type galaxy. Therefore, in order to avoid any bias from the unrealistically massive model galaxies, we show these distributions for galaxies with stellar masses in the range $10^{10}M_{\odot} < m_* < 10^{11}M_{\odot}$. We define the stellar surface density as $\log \Sigma_* = \log m_* - 2 \log r_e - \log(2\pi)$, where $r_e = 1.68r_d$. From this figure, we can readily see that if we had not excluded unstable disks, the model would have predicted a broader distribution of surface densities than is seen in the data, with a highly skewed tail to very high densities that are not observed in the disk samples. With unstable disks excluded, the width of this distribution is reasonably consistent with the data at all redshifts, though there are hints of some interesting discrepancies; namely, the observational distributions appear perhaps a bit narrower and a bit more skewed than the model predictions.

Figure 3 shows the evolution of the average value of $\log \Sigma_*$ for the same stellar mass range. As seen in the previous figure, the model predicts significant, but fairly mild, evolution in $\log \Sigma_*$ over the redshift range considered (about 0.2 dex, or about a factor of 1.5; consistent with $\Sigma_* \propto r_e^{-2}$). In Figure 3, we show the naïve scalings both for r_{200} and for r_{vir} (see §2)¹³. Both of these predict much more dramatic redshift evolution than is observed: as found in B05, and as seen here, the results from the GEMS analysis are consistent with no evolution in the average value of Σ_* over the redshift range $0.1 \lesssim z \lesssim 1.1$. B05 found that the 2- σ error bars on the average values of $\log \Sigma$ obtained from bootstrap resampling are $\sim \pm 0.04$ –0.1 dex, but this certainly underestimates the possible systematic errors. For example, the stellar mass estimates may be systematically incorrect if galaxies have more bursty star formation histories at high redshift, or the size estimates could be systematically biased by the increasingly irregular morphologies of high redshift disks (our fitting simulations assume perfectly smooth galaxies). We estimate the overall *systematic* uncertainty in size at fixed stellar mass to be $\sim 30\%$, and show representative error bars reflecting this in Figure 3. The prediction of the new model is not only a huge improvement over the naïve model, but it is in quite acceptable agreement with the GEMS data to $z \sim 1$ within these estimated uncertainties.

We now briefly explore how the models fare in comparison with the more limited data available at higher redshift. Figure 4 shows the average size of disk galaxies with stellar mass greater than $3 \times 10^{10}M_{\odot}$ predicted by the model, out to $z \sim 3$, compared with the combined results from SDSS, GEMS, and FIRE, presented by T06. Each set of points is normalized relative to the average scale length of that sample at $z = 0.1$. Results are shown for all disks, and for “stable” disks only. Note that the *absolute* average disk scale lengths for the “stable” disks are always larger than those for the total set

¹³ Note that the evolution is somewhat more rapid when the definition r_{vir} is used, because the virial overdensity used to define the halo, Δ_{vir} , evolves with redshift while with the r_{200} definition it remains constant. Because Δ_{vir} is larger at higher redshift, the halos are smaller in radius.

of disks, with no stability criterion applied, however, the redshift evolution of the stable disk sample is slightly steeper than that of the overall sample out to $z \sim 2$. This is why the stable disk sizes, when normalized relative to the average size of stable disks at $z = 0$, are a little bit lower than the total disk sample out to $z \sim 2$. We again also show the scaling for halo virial radius at fixed halo mass, which would predict much more rapid size evolution than is observed. As we have already seen, the improved model predicts fairly mild evolution in the average disk sizes out to $z \sim 1$, in quite good agreement with the GEMS data. At higher redshifts $z \sim 2$ –3, our model predicts that disks should be about 60% as large as they are today at a given stellar mass. This represents somewhat more evolution than the observational results of T06 indicate, but is within the quoted error bars.

5. DISCUSSION AND CONCLUSIONS

We have shown that a simple CDM-based model of disk formation produces good agreement with the observed weak redshift evolution of the disk size-stellar mass relation from GEMS out to $z \sim 1$. This is in contrast to the considerably stronger evolution implied by the naïve assumption that disk sizes simply scale in proportion to the dark matter halo virial radii. The reason for this more gradual evolution in the “improved” model is straightforward to understand. We can write the disk size as $r_d \propto f(f_d, c_{\text{NFW}}, \lambda) \lambda r_{\text{vir}}$, where the effect of the halo profile and adiabatic contraction are contained in the function $f(f_d, c_{\text{NFW}}, \lambda)$. Leaving aside stability considerations for the moment, this implies that any difference between the redshift evolution of the average disk sizes from that of the dark matter halo radii must be due to a systematic evolution over time in the relationship between f_d , λ , or c_{NFW} with halo mass.

In cosmological simulations, the distribution of spin parameters λ for the overall population of dark matter halos does not change with time. By construction, we have assumed that f_d is a fixed function of halo mass (though in reality this may not be true). However, simulations have shown that the halo concentration vs. mass relation *does* evolve with time: the halo concentration at fixed mass scales as $c_{\text{NFW}} \propto (1 + z)^{-1}$ (Bullock et al. 2001b). Therefore, a halo of a given mass is less concentrated at high redshift. This apparent evolution, however, is really a consequence of the way that halos are assembled in a CDM universe. Studies of the mass accretion history of halos in simulations has shown that they have two basic phases of growth: an early, rapid phase, in which the central density is set, and a second phase of more gradual accretion (Wechsler et al. 2002). The mass within the characteristic scale radius r_s is assembled during the early, rapid accretion phase. Afterwards, r_s stays nearly constant, while r_{vir} increases due to smooth accretion of mass, leading to a formal decrease in $c_{\text{NFW}} \equiv r_{\text{vir}}/r_s$. All else being equal, in our model, a less concentrated halo leads to a disk with a larger scale radius. The trend towards lower concentrations at earlier times therefore counteracts the decreased virial radii. Out to about $z \sim 1$, these competing effects nearly cancel out, leading to weak evolution in the size-mass relation.

We see a hint that the evolution predicted by these models is still a bit stronger than that indicated by the data. This could be a sign that one of the other assump-

tions in our simple model is incorrect. For example, if the disk baryon fraction f_d at a given halo mass decreases with increasing redshift, this would lead to shallower evolution and relatively larger disks at high redshift. Because we have measured the disk sizes in the rest- V band, evolving color gradients could also mask evolution in the true size of the stellar disk. Alternatively, systematic biases in our stellar mass and size estimates could be impacting the observational estimates.

We see an increasing level of discrepancy at higher redshifts, $z \gtrsim 1.5$. This could be a hint that an entirely different mechanism could be responsible for setting the sizes of disks at very high redshift. Mergers between gas-rich disks could result in a new, more spatially extended disk (Kazantzidis et al. 2005; Springel & Hernquist 2005; Robertson et al. 2006). This same scenario could also help to explain the kinematics of Damped Lyman- α systems, which are difficult to reconcile with the standard Fall-Efstathiou picture of disk formation (Maller et al. 2001).

About the same fraction of disks are classified as unstable according to the condition we adopted ($\epsilon_m < 0.75$) over the whole redshift interval $0 \leq z \leq 3$, and the exclusion of unstable disks from the sample changes the average size by nearly the same amount over this interval as well. Therefore, as implemented here, disk stability does not play a significant role in determining the relative time evolution of the stellar mass-size relation.

While the model presented here represents a significant improvement over the naïve λr_{vir} scaling frequently used in the literature, it still neglects many important aspects of disk formation in a hierarchical universe, in particular the impact of mergers. We have also ignored the possible presence of spheroids and cold gas in our disk galaxies. As well, the fraction of baryons in the disk component as a function of halo mass (f_d), here assumed to be a simple deterministic function, almost certainly has a large scatter and may change systematically with time. We intend to investigate the predictions of more detailed models, set within hierarchical merger trees, and including a full treatment of cooling, star formation, feedback, etc., in a

future work, in which we will also explore the redshift evolution of the disk size function (Somerville et al., in prep.).

ACKNOWLEDGMENTS

Based on observations taken with the NASA/ESA *Hubble Space Telescope*, which is operated by the Association of Universities for Research in Astronomy, Inc. (AURA) under NASA contract NAS5-26555. Support for the GEMS project was provided by NASA through grant number GO-9500 from the Space Telescope Science Institute, which is operated by the Association of Universities for Research in Astronomy, Inc., for NASA under contract NAS5-26555. Support for this work also came from HST Archival Grant AR-10290. SFS acknowledges financial support provided through the European Community's Human Potential Program under contract HPRN-CT-2002-00305, Euro3D RTN. EFB is supported by the DFG's Emmy Noether Program. CW was supported by a PPARC Advanced Fellowship. SJ acknowledges support from the National Aeronautics and Space Administration (NASA) under LTSA Grant NAG5-13063 issued through the Office of Space Science. DHM acknowledges support from the National Aeronautics and Space Administration (NASA) under LTSA Grant NAG5-13102 issued through the Office of Space Science. CH is supported by a CITA National Fellowship. KJ acknowledges support by the German DFG under grant SCHI 536/3-1.

Funding for the Sloan Digital Sky Survey (SDSS) has been provided by the Alfred P. Sloan Foundation, the Participating Institutions, the National Aeronautics and Space Administration, the National Science Foundation, the U.S. Department of Energy, the Japanese Monbukagakusho, and the Max Planck Society. The SDSS Web site is <http://www.sdss.org/>. The SDSS is managed by the Astrophysical Research Consortium (ARC) for the Participating Institutions. The Participating Institutions are The University of Chicago, Fermilab, the Institute for Advanced Study, the Japan Participation Group, The Johns Hopkins University, Los Alamos National Laboratory, the Max-Planck-Institute for Astronomy (MPIA), the Max-Planck-Institute for Astrophysics (MPA), New Mexico State University, University of Pittsburgh, Princeton University, the United States Naval Observatory, and the University of Washington.

REFERENCES

Avila-Reese, V., Firmani, C., & Hernández, X. 1998, ApJ, 505, 37
 Barden, M. et al. 2005, ApJ, 635, 959
 Bell, E. F., McIntosh, D. H., Katz, N., & Weinberg, M. D. 2003, ApJS, 149, 289
 Blanton, M. R. et al. 2005, AJ, 129, 2562
 Blumenthal, G., Faber, S., Flores, R., & Primack, J. 1986, ApJ, 301, 27
 Borch, A. et al. 2006, A&A, 453, 869
 Bullock, J. S., Dekel, A., Kolatt, T. S., Kravtsov, A. V., Klypin, A. A., Porciani, C., & Primack, J. R. 2001a, ApJ, 555, 240
 Bullock, J. S. et al. 2001b, MNRAS, 321, 559
 Burstein, D., Bender, R., Faber, S., & Nolthenius, R. 1997, AJ, 114, 1365
 Caldwell, J. A. R. et al. 2006, ApJ, submitted, astro-ph/0510782
 Dalcanton, J., Spergel, D., & Summers, F. 1997, ApJ, 482, 659
 Fall, S. & Efstathiou, G. 1980, MNRAS, 193, 189
 Ferguson, H. C. et al. 2004, ApJ, 600, L107
 Flores, R., Primack, J., Blumenthal, G., & Faber, S. 1993, ApJ, 412, 443
 Giavalisco, M., Steidel, C., & Macchetto, D. 1996, ApJ, 470, 189
 Governato, F. et al. 2004, ApJ, 607, 688
 Häussler, B. et al. 2006, ApJ, submitted
 Kauffmann, G. 1996, MNRAS, 281, 475
 Kazantzidis, S. et al. 2005, ApJ, 623, L67
 Kroupa, P. 2001, MNRAS, 322, 231
 Lilly, S. et al. 1998, ApJ, 500, 75
 Lowenthal, J. et al. 1997, ApJ, 481, 673
 Maller, A. H. & Dekel, A. 2002, MNRAS, 335, 487
 Maller, A. H., Prochaska, J. X., Somerville, R. S., & Primack, J. R. 2001, MNRAS, 326, 1475
 Mao, S., Mo, H. J., & White, S. D. M. 1998, MNRAS, 297, L71
 Mo, H., Mao, S., & White, S. 1998, MNRAS, 295, 319
 Navarro, J. F., Frenk, C. S., & White, S. D. M. 1997, ApJ, 490, 493
 Navarro, J. F. & Steinmetz, M. 2000, ApJ, 538, 477
 Navarro, J. F. & White, S. D. M. 1994, MNRAS, 267, 401
 Peebles, P. J. E. 1969, ApJ, 155, 393
 Pizagno, J. et al. 2006, preprint, astro-ph/0608472
 Ravindranath, S. et al. 2004, ApJ, 604, L9
 Rix, H.-W. et al. 2004, ApJS, 152, 163
 Robertson, B., Bullock, J. S., Cox, T. J., Di Matteo, T., Hernquist, L., Springel, V., & Yoshida, N. 2006, ApJ, 645, 986
 Robertson, B., Yoshida, N., Springel, V., & Hernquist, L. 2004, ApJ, 606, 32
 Shen, S. et al. 2003, MNRAS, 343, 978
 Sheth, R. K. & Tormen, G. 1999, MNRAS, 308, 119
 Simard, L. et al. 1999, ApJ, 519, 563
 Somerville, R. & Primack, J. 1999, MNRAS, 310, 1087

Sommer-Larsen, J., Gelato, S., & Vedel, H. 1999, ApJ, 519, 501
Springel, V. & Hernquist, L. 2005, ApJ, 622, L9
Syer, D., Mao, S., & Mo, H. J. 1999, MNRAS, 305, 357
Trujillo, I. et al. 2004, ApJ, 604, 521
—. 2006, ApJ, 650, 18
van den Bosch, F. C. 2000, ApJ, 530, 177

Wechsler, R. H., Bullock, J. S., Primack, J. R., Kravtsov, A. V., & Dekel, A. 2002, ApJ, 568, 52
Weil, M. L., Eke, V. R., & Efstathiou, G. 1998, MNRAS, 300, 773
Wolf, C. et al. 2004, A&A, 421, 913